

## Supporting Information

### Wedge Dyakonov Waves and Dyakonov Plasmons in Topological Insulator $\text{Bi}_2\text{Se}_3$ Probed by Electron Beams

*Nahid Talebi,<sup>†</sup> Cigdem Ozsoy-Keskinbora,<sup>†</sup> Hadj M. Benia,<sup>†</sup> Klaus Kern,<sup>†‡</sup> Christoph T. Koch,<sup>§</sup> Peter A. van Aken<sup>†</sup>*

<sup>†</sup>Max Planck Institute for Solid State Research, D–70569 Stuttgart, Germany

<sup>‡</sup>Institut de Physique de la Matière Condensée, Ecole Polytechnique Fédérale de Lausanne, 1015 Lausanne, Switzerland

<sup>§</sup>Humboldt University of Berlin, Department of Physics, 12489 Berlin, Germany

#### Contents:

- 1- Evanescent modes at the interface of a uniaxial anisotropic and an isotropic medium
- 2- EFTEM images for several  $\text{Bi}_2\text{Se}_3$  particles
- 3- Complete Band diagram of a  $\text{Bi}_2\text{Se}_3$  rib waveguide

## 1- Evanescent modes at the interface of a uniaxial anisotropic and an isotropic medium

In order to obtain the characteristic equations for the slab waveguide shown in Figure S1, a vector-potential approach is utilized. This approach helps us to more efficiently distinguish and derive the possible modal groups, rather than the usual approach to construct the solutions at the field level.<sup>1, 2</sup> This is because that in contrast to the field approach one can derive a Helmholtz equation for vector potentials even for an anisotropic medium, though such an equation is not valid for field components in general. We first consider the Maxwell equations as:

$$\vec{\nabla} \times \vec{E}(\vec{r}, \omega) = -i\omega \vec{B}(\vec{r}, \omega) \quad (1a)$$

$$\vec{\nabla} \times \vec{H}(\vec{r}, \omega) = i\omega \vec{D}(\vec{r}, \omega) \quad (1b)$$

$$\vec{\nabla} \cdot \vec{B}(\vec{r}, \omega) = 0 \quad (1c)$$

$$\vec{\nabla} \cdot \vec{D}(\vec{r}, \omega) = 0 \quad (1d)$$

where the harmonic representation as  $\exp(i\omega t)$  is considered, with  $i^2 = -1$ . We consider also the constitutive relations including the ME effect as:

$$\vec{D}(\vec{r}, \omega) = \varepsilon_0 \hat{\varepsilon}_r(\omega) : \vec{E}(\vec{r}, \omega) \quad (2a)$$

$$\vec{H}(\vec{r}, \omega) = \frac{1}{\mu_0} \vec{B}(\vec{r}, \omega) \quad (2b)$$

Since the magnetic flux density  $\vec{B}(\vec{r}, \omega)$  is a pure solenoidal vector quantity it can be described as the curl of another vector, which is called the magnetic vector potential, as:

$$\vec{B} = \vec{\nabla} \times \vec{A} \quad (3)$$

in which we have dropped the argument  $(\vec{r}, \omega)$  for simplicity. Inserting eq. (3) in eq. (1a) gives:

$$\vec{E} = -i\omega \vec{A} - \vec{\nabla} \varphi \quad (4)$$

in which  $\varphi$  is the electric scalar potential. Using (1) to (4), we can derive the following equation for the magnetic vector potential:

$$\begin{aligned} \frac{1}{\mu_0} \left( \vec{\nabla} \vec{\nabla} \cdot \vec{A} - \nabla^2 \vec{A} \right) - \omega^2 \varepsilon_0 \hat{\varepsilon}_r : \vec{A} + \\ i\omega \varepsilon_0 \hat{\varepsilon}_r : \vec{\nabla} \varphi = 0 \end{aligned} \quad (5)$$

Equation (3) only defines the rotational part of the magnetic vector potential. We are free to employ a gauge theory to fix its solenoidal part. In order to do so, we can define a generalized Lorentz gauge in the form of:

$$\vec{\nabla} \varphi = \frac{-\hat{\varepsilon}_r^{-1}}{i\omega \varepsilon_0 \mu_0} \vec{\nabla} \vec{\nabla} \cdot \vec{A} \quad (6)$$

Using (6), (5) is further simplified to a Helmholtz equation in the form of:

$$\nabla^2 \vec{A} + k_0^2 \hat{\varepsilon}_r : \vec{A} = 0 \quad (7)$$

in which  $k_0 = \omega\sqrt{\varepsilon_0\mu_0}$  is the wave vector of the light in free space. Solutions to (7) are called wave potentials. The field components obtained using eqs. (3), (4) and (6).

We consider here the solutions to the optical modes excited at the interface of a uniaxial anisotropic material and an isotropic dielectric located at  $z \leq 0$  and  $z \geq 0$ , respectively. The optic axis is parallel to the interface, and without any loss of generality we consider the wave to propagate along the  $x$ -axis and evanescent along the  $z$ -axis. Moreover, the only non-zero elements of the permittivity tensor are  $\varepsilon_{rxx} = \varepsilon_{ryy} = \varepsilon_{r\parallel}$  and  $\varepsilon_{rzz} = \varepsilon_{r\perp}$ . The optical modes in such a system are decomposed into two individual sets; namely  $\text{TM}_x$  and  $\text{TM}_z$ , where they are constructed by the choice of the magnetic vector potential as  $\vec{A} = (A_x, 0, 0)$  and  $\vec{A} = (0, 0, A_z)$ , respectively. It is easily verified that a choice as  $\vec{A} = (0, A_y, 0)$  will not satisfy the boundary conditions. For each case, the solutions to wave potentials can be constructed as  $A_\alpha(\vec{r}, \omega) = \tilde{A}_\alpha^+ \exp(-\kappa_z^{(d)} z) \times \exp(-i\beta z)$  and  $A_\alpha(\vec{r}, \omega) = \tilde{A}_\alpha^- \exp(\kappa_z^{(2,\alpha)} z) \exp(-i\beta z)$  for  $z \geq 0$ , and  $z \leq 0$ , respectively, where  $\beta = \beta' - i\beta''$  is the propagation constant ( $\beta'$  is the phase constant and  $\beta''$  is the attenuation constant),  $(\kappa_z^{(2,\alpha)})^2 = \beta^2 - \varepsilon_{r\alpha\alpha} k_0^2$  and  $(\kappa_z^{(d)})^2 = \beta^2 - \varepsilon_{rd} k_0^2$ . Moreover,  $\alpha \in (x, z)$ .

We first consider solutions to the  $\text{TM}_x$  modes. Satisfying the tangential boundary conditions for the  $E_x$  and  $H_y$  field components, the propagation constant of the optical modes at the interface is obtained as:

$$\beta^{\text{TM}_x} = \pm \sqrt{\varepsilon_{rd}} k_0 \sqrt{\varepsilon_{r\parallel} / (\varepsilon_{r\parallel} + \varepsilon_{rd})} \quad (8)$$

Interestingly, only it is only the  $\varepsilon_{r\parallel}$  component of the permittivity which affect the propagation constant of the  $\text{TM}_x$  mode. Moreover, eq. (8) is quite similar to the propagation constant of plasmon polaritons at the interface of two isotropic materials with the relative permittivity of  $\varepsilon_{r\parallel}$  and  $\varepsilon_{rd}$ , respectively. In order to have evanescent modes, the real parts of  $\kappa_z^{(2,x)}$  and  $\kappa_z^{(d)}$  should be positive, which lead us to the criterion  $\varepsilon_{r\parallel} < -\varepsilon_{rd}$ . This means that in order to have evanescent  $\text{TM}_x$  modes, the material should be metallic at least in the direction of the optic axis.

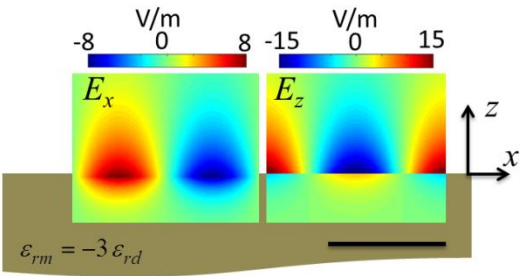
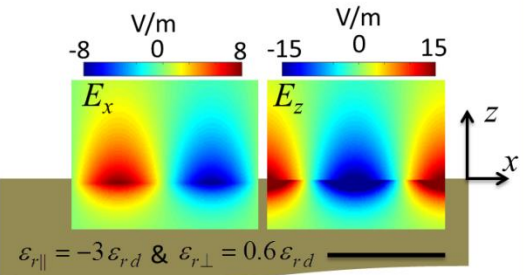
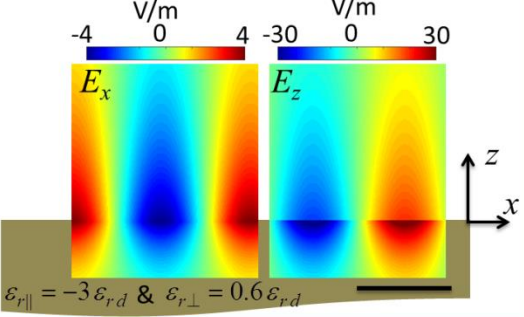
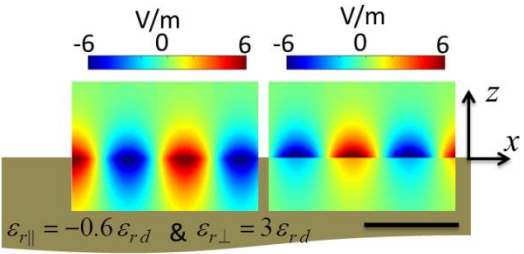
The propagation constant for the  $\text{TM}_z$  mode can be derived as:

$$\beta^{\text{TM}_z} = \pm \sqrt{\varepsilon_{rd}} k_0 \sqrt{(\varepsilon_{r\parallel}^2 - \varepsilon_{rd} \varepsilon_{r\perp}) / (\varepsilon_{r\parallel}^2 - \varepsilon_{rd}^2)} \quad (9)$$

In order to have bound  $\text{TM}_z$  modes, the real parts of the damping factors  $\kappa_z^{(2,z)}$  and  $\kappa_z^{(d)}$  should be positive, which leads to more difficult criterion, as shown in table S1.

The last criterion (C4) for  $TM_z$  modes has been so far considered in the literature<sup>1</sup> as the criterion to excite the bound Dyakonov mode at the interface of uniaxial anisotropic/isotropic materials, as  $\epsilon_{r\parallel} < \epsilon_{rd} < \epsilon_{r\perp}$ , when both  $\epsilon_{r\parallel}$  and  $\epsilon_{r\perp}$  can be positive. Moreover for  $\epsilon_{r\parallel} < -\epsilon_{rd}$  and  $\epsilon_{r\perp} < \epsilon_{rd}$

**Table S1.** Bound modes at the interfaces of isotropic/isotropic and anisotropic/isotropic materials. Scale bar is  $2\pi/\sqrt{\epsilon_{rd}} k_0$ .

	Propagation constant	Criterion for bound modes	Field profile
Isotropic material	$\beta = \sqrt{\epsilon_{rd}} k_0 \times \sqrt{\frac{\epsilon_{rm}}{\epsilon_{rm} + \epsilon_{rd}}}$	C1 $\frac{\epsilon_{rm}}{\epsilon_{rd}} < -1$	
Anisotropic uniaxial material	TM <sub>x</sub> modes $\beta = \sqrt{\epsilon_{rd}} k_0 \times \sqrt{\frac{\epsilon_{r\parallel}}{\epsilon_{r\parallel} + \epsilon_{rd}}}$	C2 $\frac{\epsilon_{r\parallel}}{\epsilon_{rd}} < -1$	
	TM <sub>z</sub> modes $\beta = \sqrt{\epsilon_{rd}} k_0 \times \sqrt{\frac{(\epsilon_{r\parallel}^2 - \epsilon_{rd} \epsilon_{r\perp})}{(\epsilon_{r\parallel}^2 - \epsilon_{rd}^2)}}$	C3 $\left( \left  \frac{\epsilon_{r\parallel}}{\epsilon_{rd}} \right  > 1 \right. \\ \left. \& \frac{\epsilon_{r\perp}}{\epsilon_{rd}} < 1 \right)$  C4 $\left( \left  \frac{\epsilon_{r\parallel}}{\epsilon_{rd}} \right  < 1 \right. \\ \left. \& \frac{\epsilon_{r\perp}}{\epsilon_{rd}} > 1 \right)$	 

both  $TM_x$  and  $TM_z$  modes can be excited, even if  $\varepsilon_{r\perp} > 0$ , for which the material is called hyperbolic. Interestingly, whereas the only non-zero field components for both  $TM_x$  and  $TM_z$  modes are  $E_x$ ,  $E_z$ , and  $H_y$ , the field profiles are different as shown in table S1, and the overall polarization state would be different for these cases. Notably for an isotropic/isotropic interface,  $TM_z$  and  $TM_x$  modes are degenerate.

All the criteria above are only valid for lossless materials. However, for real materials, the dielectric loss is not negligible as the imaginary part of the permittivity can be even larger than the real part, especially at the energies near to the inter band transitions, as happens also for  $Bi_2Se_3$  material. For the sake of completeness for our discussions regarding the interface modes, we have computed here the propagation constants of the optical modes at the interface of  $Bi_2Se_3$ /air and  $Bi_2Se_3$ /a-C, where a-C stands for amorphous carbon.

As noted in the main text,  $Bi_2Se_3$  has three distinguished energy ranges: It is dielectric at  $E < 1.06$  eV, hyperbolic type I ( $\varepsilon_{r\perp} < 0$  and  $\varepsilon_{r\parallel} > 0$ ) at  $1.06$  eV  $< E < 1.73$  eV, and hyperbolic type II ( $\varepsilon_{r\perp} > 0$  and  $\varepsilon_{r\parallel} < 0$ ) at  $E > 1.73$  eV. These frequency ranges are denoted by  $\mathcal{D}$ ,  $\mathcal{H}$  II, and  $\mathcal{H}$  I respectively. both  $TM_x$  and  $TM_z$  modes can be excited in the whole frequency range at the

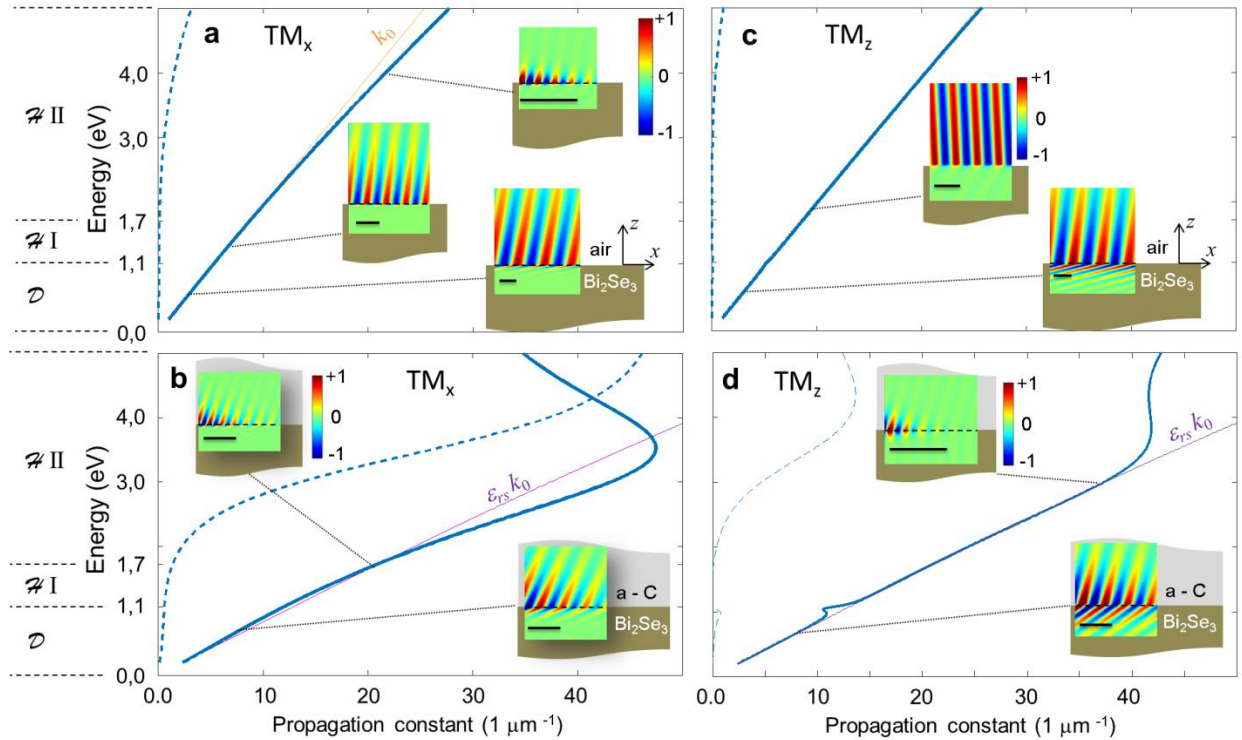


**Figure S1:** Propagation constant of a)  $TM_x$  mode at  $Bi_2Se_3$ /air, b)  $TM_z$  mode at  $Bi_2Se_3$ /air for c)  $TM_x$  modes at  $Bi_2Se_3$ /a-C, and d) a)  $TM_z$  modes at  $Bi_2Se_3$ /a-C interfaces. Spatial field distribution for  $E_x$  field component at a given time and selected energies are depicted at the insets.

Bi<sub>2</sub>Se<sub>3</sub>/air interface, while there is a clear gap at the excitation energies of the forwardly propagating ( $\beta^{\text{TM}_z} = +\sqrt{\epsilon_{rd}} k_0 \sqrt{(\epsilon_{r\parallel}^2 - \epsilon_{rd} \epsilon_{r\perp}) / (\epsilon_{r\parallel}^2 - \epsilon_{rd}^2)}$ , see eq. (9)) TM<sub>z</sub> modes, as attenuation constant becomes negative in some energy ranges. At these energies, a backwardly propagating mode ( $\beta^{\text{TM}_z} = -\sqrt{\epsilon_{rd}} k_0 \sqrt{(\epsilon_{r\parallel}^2 - \epsilon_{rd} \epsilon_{r\perp}) / (\epsilon_{r\parallel}^2 - \epsilon_{rd}^2)}$ , see eq. (9)) with a negative phase velocity is still possible, which can only be excited at discontinuities and tapers<sup>3</sup>. Moreover, despite the case of isotropic plasmons in a Drude metal like silver or aluminum, the hyperbolic plasmon dispersion in Bi<sub>2</sub>Se<sub>3</sub> are in general more attached to the light line, due to the huge dielectric loss.

## 2- EFTEM images for several Bi<sub>2</sub>Se<sub>3</sub> particles

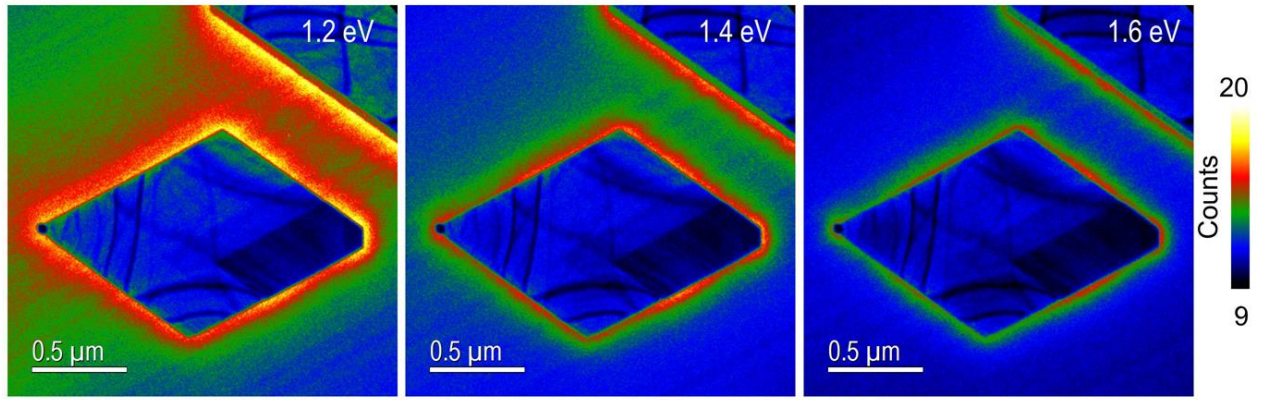


**Figure S2:** shows the EFTEM series for a Bi<sub>2</sub>Se<sub>3</sub> particle with the thickness of 55 nm positioned on a carbon substrate, which supports wedge modes.

## Complete Band diagram of a Bi<sub>2</sub>Se<sub>3</sub> rib waveguide

In order to emphasize the extremely huge number of PDOS in the Bi<sub>2</sub>Se<sub>3</sub> rib waveguide, the full photonic dispersion diagram as well as the computed PDOS is demonstrated in Figure S3. In order to calculate the PDOS from the numerical data, the method described in ref. 4 is used.

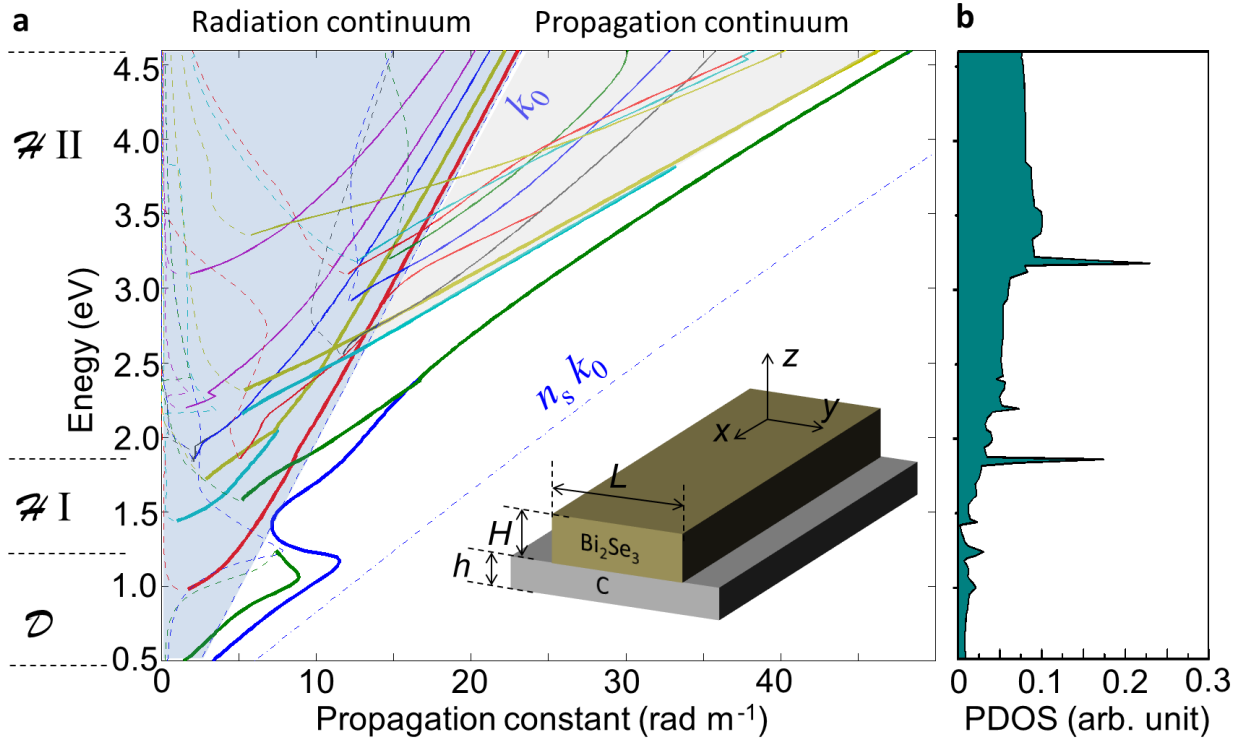


**Figure S3:** (a) Dispersion diagram and (b) photonic local density of states (PDOS) sustained by a Bi<sub>2</sub>Se<sub>3</sub> rib waveguide on a amorphous carbon substrate.  $L = 400$  nm,  $H = 50$  nm, and  $h = 55$  nm.

## References

1. Polo, J. A.; Lakhtakia, A., Surface Electromagnetic Waves: A Review. *Laser Photonics Rev.* **2011**, 5, 234-246.
2. Walker, D. B.; Glytsis, E. N.; Gaylord, T. K., Surface Mode at Isotropic-Uniaxial and Isotropic-Biaxial Interfaces. *J. Opt. Soc. Am. A* **1998**, 15, 248-260.
3. Jang, M. S.; Atwater, H., Plasmonic Rainbow Trapping Structures for Light Localization and Spectrum Splitting. *Phys. Rev. Lett.* **2011**, 107, 207401.
4. Busch, K.; John, S., Photonic Band Gap Formation in Certain Self-Organizing Systems. *Phys. Rev. E* **1998**, 58, 3896-3908.